Original Articles

New drought index indicates that land surface changes might have enhanced drying tendencies over the Loess Plateau

Meixian Liu[a,b], Xianli Xu[a,b,*], Alexander Y. Sun[c]

[a] Key Laboratory for Agro-ecological Processes in Subtropical Region, Institute of Subtropical Agriculture, Chinese Academy of Sciences, Changsha 410125, PR China
[b] Huanjiang Observation and Research Station for Karst Ecosystem, Chinese Academy of Sciences, Huanjiang 547100, PR China
[c] Bureau of Economic Geology, Jackson School of Geosciences, The University of Texas at Austin, Austin, TX, USA

A B S T R A C T

To prevent soil erosion and improve ecological environment over the Loess Plateau, the Chinese Government implemented a large scale ecological restoration (ER) in the past decades. ER activities have successfully reduced soil erosion and expanded vegetation, and also changed the water-energy balance, which would alter the hydrological dryness conditions. Knowledge of the impacts of land surface changes on hydrological dryness is essential for ER-related policy making and management. However, so far few studies have addressed this important issue. Thus, this study aimed to evaluate the effects of land surface changes on hydrological dryness in 13 main catchments in the Loess Plateau during 1961–2009, based on the standardized wetness index (SWI), which can be used to measure the hydrological dryness resulting from climate change solely (denoted as SWI_c) and from the joint effects of climate and land surface changes (denoted as SWI_{cl}). Statistical analysis (correlation $r > 0.80$) demonstrated that the land surface changes, being represented by the LIM (total affecting area of terrace and check-dams), RM (total affecting area of replanted trees and pastures), LAI (leaf area index), and VC (vegetation coverage), dominated the behaviors of n (a parameter of the Budyko-type formulae). The overall increasing n indicated that more and more water from precipitation becomes evapotranspiration in the past decades. Furthermore, both the SWI_c and SWI_{cl} decreased; however, the trend in SWI_{cl} was $(-2.7 \pm 0.76) \times 10^{-3}\,\text{month}^{-1}$, being visibly larger than that of SWI_c $((-1.3 \pm 0.65) \times 10^{-3}\,\text{month}^{-1})$. These suggested that the Loess Plateau was becoming drier, while the land surface changes might have enhanced the drying tendencies.

1. Introduction

The Loess Plateau (LP), located in the middle reaches of the Yellow River (YR) Basin, accounts for nearly 90% of the total sediment in the YR (Zhao et al., 2014). To prevent soil erosion and protect the vulnerable ecological environment, numerous ecological restoration (ER) measures have been implemented over the LP in the past half-century. Especially in the late 1990s, a large reforestation campaign named the "Grain-for-Green (GFG)" program, was carried out (Feng et al., 2012; McVicar et al., 2007a; Wang et al., 2015b). These ER activities, mainly including afforestation, pasture reestablishment, terraces and check-dams construction (Wang et al., 2015b; Zhang et al., 2008b), have led to visible expansion of vegetation (Zhang et al., 2016a), reduction in soil erosion (Wang et al., 2015b) and increase in infiltration (Chen et al., 2015; Zhang et al., 2014). Besides these, the significantly modified land surface also altered the water balance (Liang et al., 2015;

Zhang et al., 2016a, 2008b), which is critical for the security of water resources and ecological environment.

Many studies focused on the hydrological effects of the ER activities over the LP in recent years. For example, Liang et al. (2015) found that the contribution of ER (62%) to runoff reduction was much larger than that of climate change (38%). Zhang et al. (2014) reported that 74% of the reduction in runoff could be attributed to the ER activities in a small catchment on the LP. Feng et al. (2012) pointed out that water yield in 38% (area) of the LP decreased due to the land cover changes. Also, based on a water balance model, Zhang et al. (2008a) predicted that runoff would decrease by 5.5% and 9.2%, if 5.8 and 10.1% of the LP were planted with trees. Clearly, these existing studies mainly evaluated the hydrological effects of ER activities based on runoff (water yield) (Gao et al., 2015; Liang et al., 2015; Zhang et al., 2014, 2008a; Zhao and Yu, 2013).

However, any change in runoff came as a result of water balance/

---

storage changes. Exactly, ER activities not only improved soil-water conservation (increased infiltration and reduced runoff), but also changed the ecological water consumption (Wang et al., 2015b; Zhao et al., 2014), and would consequently alter the dry and wet conditions. For instance, if the increase in infiltration due to ER activities can't compensate for the increase in water consumption, then a drier environment would be formed. Indeed, there existing literature pointed out that soil water storage (in 400 mm soil layer) in the artificial revegetated lands was lower than those in bare land and natural restored land over the LP (Zeng et al., 2011). Compared to runoff, dryness may have closer relationship with vegetation (Zhao and Running, 2010). The altered dryness should in turn affect the growth of vegetation, and exert important impacts on the sustainability of the reconstructed ecosystem. Hence, evaluating the impacts of ER activities (land surface changes) on dryness is essential for ER planning and ecosystem management in this region.

Drought indices are effective tools in quantifying dryness/wetness conditions (Dai, 2011), which are closely related to vegetation production and runoff (Vicente-Serrano and Lopez-Moreno, 2005; Zhao and Running, 2010). There exist many drought indices, such as the Palmer Drought Severity Index (PDSI) (Palmer, 1965), Standardized Precipitation Index (McKee et al., 1993), Standardized Precipitation Evapotranspiration Index (SPEI) (Vicente-Serrano et al., 2010), which are widely used in monitoring and assessing droughts over the globe, including the LP or the YR Basin (Wang et al., 2015a; Zhang et al., 2016a, 2013, 2012; Zhao and Wu, 2013). However, these drought indices are not applicable in evaluating the impacts of land surface changes on dryness (Liu et al., 2017).

More recently, Liu et al. (2017) proposed a new hydrological drought index, the Standardized Wetness Index (SWI), based on the Budyko framework (Budyko, 1974; Choudhury, 1999) and the structure of SPEI (Vicente-Serrano et al., 2010). The SWI can represent the hydrological dryness/wetness resulting from climate change (variability) solely, and from the joint effects of climate and land surface changes (variability), and hence provides a potential means to evaluate the relative impacts of climate and land surface changes (variability) on hydrological dryness (Liu et al., 2017). This study mainly aimed to 1) investigate the effects of land surface changes on the Budyko-type water balance (parameter n in Eq. (2) below), and 2) to evaluate the effects of the land surface changes on hydrological dryness over LP by using SWI. The results would be helpful in water resources management and ecosystem reconstruction, maintenance and protection over the LP.

2. Data and methods

2.1. Brief description of the standardized wetness index (SWI)

The SWI (dimensionless) is based on a residual water-energy ratio (WER, dimensionless):

$$WER = \frac{P-E}{ET_0-E} \qquad (1)$$

where P, E, and ET_0 represent precipitation, actual evaporation, and potential evaporation, respectively. In the ratio $\frac{P-E}{ET_0-E}$, E is estimated using the Choudhury's equation (Budyko, 1974; Choudhury, 1999):

$$E = \frac{P \cdot ET_0}{(p^n + ET_0^n)^{1/n}} \qquad (2)$$

where n is generally considered a catchment-dependent property that reflects the interactions between land surface and atmosphere (Liu et al., 2017). Because the Budyko hypothesis is not applicable at short time scales (e.g. sub-annual scale), the SWI can only be derived for relatively long-term scale (e.g. longer than 12-month). To do this, the SWI uses a moving average approach to aggregate P, E, and ET_0 at relatively long-term scale. For example, in calculating the 12-month scale WER for $month_i$, the mean P, E, and ET_0 in the period from

$month_{i-11}$ to $month_i$ are used. And in calculating the 24-month scale WER for $month_i$, the mean P, E, and ET_0 in the period from $month_{i-23}$ to $month_i$ are used. The SWI is obtained by standardizing the WER series using the three-parameter log-logistic distribution, like the SPEI (Vicente-Serrano et al., 2010). Similar to the SPEI, negative and positive values of SWI indicate, respectively, drier and wetter than normal conditions. The effectiveness of SWI in drought monitoring has been validated at the global scale (Liu et al., 2017).

Most importantly, there are two features of SWI, based on different types of n (static or dynamic) (Liu et al., 2017). It is well known that water-energy balance is affected by many factors, including the climatic properties (e.g. climate seasonality, such as precipitation variation and distribution, snow) and land surface properties (e.g. human activities, soil water capacity, vegetation) (Donohue et al., 2010; Liu et al., 2017; Zhang et al., 2016b). In the simple Budyko-type water balance, the effects of these factors on water balance can only be reflected by the parameter n, because the other two variables are just the total amount of P and ET_0. Therefore, when using dynamic n (considers the effects of land surface and climate seasonality) to derive SWI, then this SWI considers the joint effects of climate and land surface changes (variability) (denoted as SWI_{cl}); and when using static n (ignores the effects of land surface and climate seasonality) to derive SWI, then the SWI only considers climate change (variability) (denoted as SWI_c).

2.2. Study area

The Loess Plateau (LP) (Fig. 1), has an arid and semiarid continental monsoon climate (Table 1) (McVicar et al., 2007b). Precipitation mainly occurs from June to September. In this study, 12 main tributaries (Fig. 1b) and the catchment between the Toudaoguai and Huayuankou (abbreviated to be TDG-HYK) (Fig. 1c) were selected, within which the TDG-HYK was used to represent the entire LP (Fig. 1c). These 13 water-limited catchments (Fig. 2) cover the major part of the LP (Fig. 1c). Details of these catchments are presented in Table 1. Note that in the TDG-HYK, the human water consumption (e.g. extraction from river, reservoir and etc.) accounts for a very small part of the annual precipitation (about 1.0%), though it increased in the past decades (from 0.5% in 1950s to 1.4% in 1990s) due to the growing population, industrialization and urbanization (Wang et al., 2002). Therefore, the human water consumption may be relatively ignorable in this region.

2.3. Data sources

Long-term annual runoff (Q, mm year^{-1}) (1961–2009) data were collected from the Yellow River Conservancy Commission (http://www.yellowriver.gov.cn/). Daily meteorological data from 1961 to 2009 at 61 meteorological stations (Fig. 1c) were collected from the China Meteorological Data Service Network (http://www.escience.gov.cn/metdata/page/index.html). The catchment scale annual mean soil moisture (SM), which was used to evaluate the effectiveness of SWI, was derived based on the Climate Change Initiative Soil Moisture dataset (CCI SM V02.2) collected from European Space Agency (ESA) (http://www.esa-soilmoisture-cci.org/node/145). The CERES EBAF Surface Fluxes data set (Ed 2.8, 1° × 1° grid, 2000–2014) (http://ceres.larc.nasa.gov/order_data.php) was used to calibrate the surface albedo in calculating potential evaporation. To reflect the land surface changes, vegetation coverage, leaf area index and the cumulative affecting area (km^2) of ER measures were used. In particular, the cumulative affecting area (km^2) of ER measures, including terraces, check dams, tree and grass planting, were collected from Liang et al. (2015), Yao et al. (2011) and Wang and Fan (2002). These data are available for 1969, 1979, 1989, 1999, and 2006. The vegetation coverage was calculated based on the GIMMS NDVI3g $NDVI$ (1982–2012) (Anyamba et al., 2014), and the leaf area index (LAI) data were collected from the Global Inventory Modelling and Mapping Studies-Advanced Very High
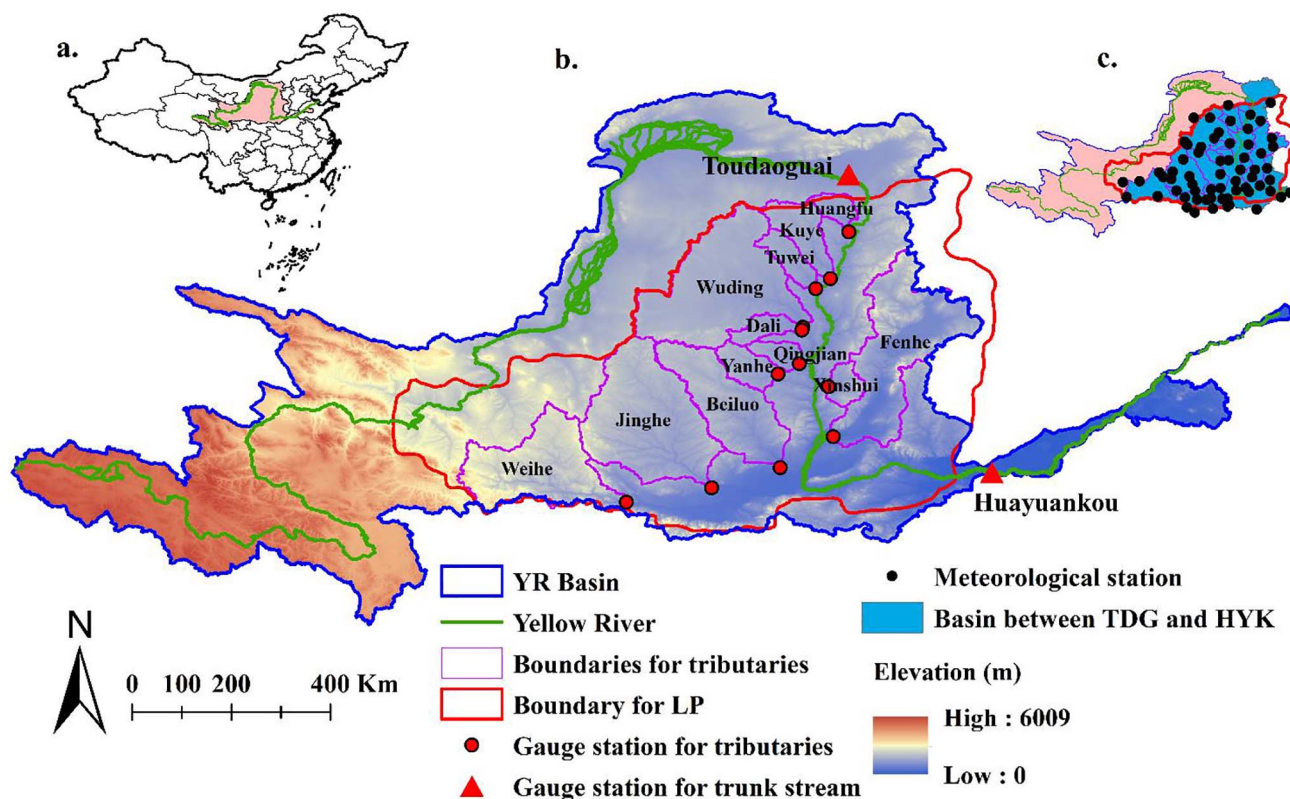
Fig. 1. Map for the study region. (a) Location of the Yellow River Basin in China; (b) distribution of the selected 12 tributaries (pink polygons), the location of the Loess Plateau (the red polygon) and hydrometrical stations (red dots and red triangles); (c) the catchment between the Toudaoguai and Huayuankou hydrometrical stations (the blue colored region) and the distribution of meteorological stations (black dots). (For interpretation of the references to colour in this figure legend, the reader is referred to the web version of this article.)

Resolution Radiometer (GIMMS AVHRR) (http://www.glcf.umd.edu/data/lai/).

2.4. Determining SWI_c and SWI_cl

In this study, the SWI_c and SWI_{cl} were derived at 12-month scale. First, 12-month scale precipitation (P_i^{12}, mm $(12\text{-month})^{-1}$) and potential evaporation (ET_{0i}^{12}, mm $(12\text{-month})^{-1}$) for $month_i$ were aggregated for calculating the 12-month scale residual water-energy ratio (WER_i^{12}):

$$P_i^{12} = \sum_{i-11}^{i} P_i \tag{3}$$

$$ET_{0i}^{12} = \sum_{i-11}^{i} ET_{0i} \tag{4}$$

$$WER_i^{12} = \frac{P_i^{12}}{ET_{0i}^{12}} \frac{((P_i^{12})^n + (ET_{0i}^{12})^n)^{1/n} - ET_{0i}^{12}}{((P_i^{12})^n + (ET_{0i}^{12})^n)^{1/n} - P_i^{12}} \tag{5}$$

where P_i^{12} and ET_{0i}^{12} are the 12-month scale precipitation and potential evaporation in $month_i$. Note that here the potential evaporation was estimated using the Penman method (Penman, 1948), within which the solar radiation was estimated using the Angstrom equation (Allen et al., 1998) and the surface albedo was calibrated using the CERES EBAF Surface Fluxes dataset. Details can be found in (Liu et al., 2016a).

To derive the SWI_c, the static n (denoted as n_s) was determined by numerically solving Eq. (6) based on the long-term mean annual P, ET₀ and Q in 1961–2009:

Table 1
Main long-term hydrometeorological characteristics of the 13 selected catchments.

| No.	Catchments	Gauge station	Area (10^4 km²)	P (mm year^{-1})	Aridity index	Q (mm year^{-1})	Rc[*]	n
1	Huangfu	Huangfu	0.32	400.1	2.6	37.0	0.09	1.75
2	Kuye	Wenjiachuan	0.86	371.7	3.1	60.1	0.16	1.24
3	Tuwei	Gaojiachuan	0.33	379.8	2.9	88.7	0.23	1.05
4	Wuding	Dingjiagou	2.47	344.8	3.3	34.9	0.10	1.47
5	Dali	Suide	0.39	399.6	3.0	36.6	0.09	1.63
6	Qingjian	Yanchuan	0.36	508.1	2.0	38.3	0.08	2.29
7	Yanhe	Ganguyi	0.59	530.8	2.0	34.0	0.06	2.44
8	Beiluo	Zhuangtou	2.57	490.0	2.2	35.0	0.07	2.17
9	Jinghe	Zhangjiashan	4.31	489.9	2.1	33.1	0.07	2.30
10	Weihe	Linjiacun	3.01	541.7	1.7	65.4	0.12	2.18
11	Fenhe	Hejin	3.87	460.5	2.4	22.6	0.05	2.34
12	Xinshui	Daning	0.42	517.7	2.1	29.5	0.06	2.47
13	TDG-HYK	Toudaogui-Huayuankou	36.21	480.1	2.3	40.3	0.08	2.00

[*] Runoff coefficient = Q/P.
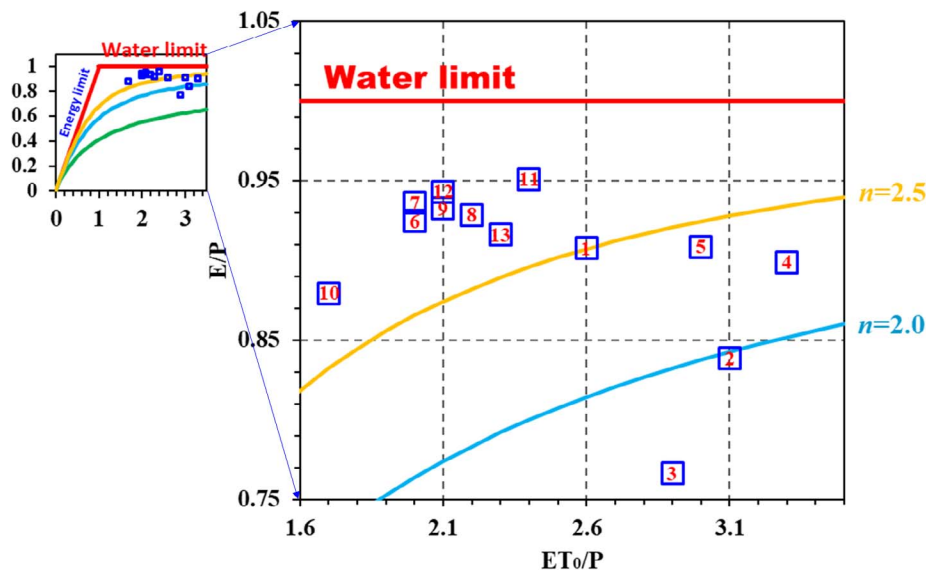
Fig. 2. Relationship between long-term averaged E/P and ET$_0$/P for the 13 catchments over the LP, the catchment number is provided in Table 1.

$$E = (P - Q) = \frac{P \cdot ET_0}{(P^n + ET_0^n)^{1/n}} \tag{6}$$

Then this n_s was used in Eq. (5) to calculate the WER_{si}^{12} series (WER_{si}^{12} means the WER_i^{12} that derived using static n_s). In calculation of SWI_{cl}, the dynamic n (denoted as n_d, dimensionless) was estimated by using six relative long-term moving windows (5-, 6-, 7-, …10-year moving windows), for minimizing the effects of water storage changes (Donohue et al., 2013; Liu et al., 2017; Yang et al., 2016). In this procedure, when n_d is calculated for $month_i$ and $month_{i-11}$ is a month in 1961 (regardless of whatever the month is), then the mean annual P, ET$_0$ and Q in the periods of 1961–1965, 1961–1966, 1961–1967, 1961–1968, 1961–1969 and 1961–1970, were used to calculate the n_d^5, n_d^6, n_d^7, n_d^8, n_d^9, and n_d^{10} (n_d^5 means the n_d is estimated by 5-year mean P, ET$_0$ and Q), respectively. The same approach was used in other months. Liu et al. (2017) demonstrated the effectiveness of this dynamic n estimation method. These estimated n_d values were substituted into Eq. (5) to derive the WER_{di}^{12}, which were denoted as WER_{d5i}^{12}, WER_{d6i}^{12}, WER_{d7i}^{12}, WER_{d8i}^{12}, WER_{d9i}^{12}, and WER_{d10i}^{12} (WER_{d5i}^{12} means the WER_{di}^{12} derived based on n_d^5). It is important to note that for all the months in the last window, we used the same n_d derived based on the mean P, ET_0 and Q in the last window. For example, when calculating the WER_{d5i}^{12} for all the months in 2005–2009, we use the n_d^5 derived in 2005–2009.

Thereafter, based on the WER_{si}^{12} series, the three-parameter log-logistic distribution (denoted as $LLD3_s$) was determined (Vicente-Serrano et al., 2010) and was used to calculate the SWI_c. Meanwhile, the same $LLD3_s$ used for SWI_c was used to standardize the six WER_{di}^{12} series for producing SWI_{cl} (denoted as SWI_{cl5}, SWI_{cl6}, SWI_{cl7}, SWI_{cl8}, SWI_{cl9}, and SWI_{cl10}, respectively).

2.5. Relationships between parameter n and land surface changes

The SWI provides a potential means to evaluate the effects of land surface changes on hydrological dryness (Liu et al., 2017). However, the relationship between n and land surface properties need to be quantified first. In this study, the land surface changes were reflected by the cumulative affecting area of ER measures, leaf area index (LAI), and vegetation coverage (VC):

$$VC = \frac{NDVI - NDVI_{min}}{NDVI_{max} - NDVI_{min}} \tag{7}$$

where the $NDVI_{min}$ and $NDVI_{max}$ were chosen to be 0.05 and 0.8 (Li et al., 2013). In particular, the ER measures were classified into two types, the land improvement measures (LIM, total cumulative affecting

area of terrace and check dams) and the replanting measures (RM, total cumulative affecting area of replanted trees and grass).

Correlation analysis was conducted between the dynamic n and land surface properties (LIM, RM, VC and LAI). Note that the cumulative affecting area of LIM (terrace and check dams) and RM (tree and grass) were available for 1969, 1979, 1989, 1999 and 2006. In the analysis, the LIM and RM were used as the independent variables, and the n_d^{10} derived in the periods of 1965–1974, 1975–1984, 1985–1994, 1995–2004 and 2000–2009 were the dependent variables. As for the VC and LAI, the time series were artificially divided into 5 periods (every 5 years): 1982–1986, 1987–1991, 1992–1996, 1997–2001 and 2002–2006. Then, the mean VC and LAI in the 5 periods were the independent variables, and the n_d^5 derived in the same periods (exactly in 1982–1986, 1987–1991, 1992–1996, 1997–2001 and 2002–2006) were the dependent variables.

2.6. Statistical analysis

The trends of n_d (n_d^5, n_d^6, n_d^7, n_d^8, n_d^9, and n_d^{10}), SWI_c and SWI_{cl} (SWI_{cl5}, SWI_{cl6}, SWI_{cl7}, SWI_{cl8}, SWI_{cl9}, and SWI_{cl10}) were examined using the modified pre-whitening Mann–Kendall trend test (Kendall, 1975; Mann, 1945; Yue and Wang, 2002). The magnitudes of these trends were estimated as follows (Burn and Elnur, 2002; Yang et al., 2014):

$$\theta = Median\left[\frac{x_j - x_i}{j - i}\right] 1 < i < j < K \tag{8}$$

where θ is the magnitude of the trend, and x_i and x_j are the i-th and j-th observations, respectively; and K is the length of the series. Meanwhile, correlation analysis was also performed among the annual SWI_c, SWI_{cl}, Q and soil moisture (SM) for evaluating the effectiveness of SWI in detecting dry and wet conditions.

3. Results

3.1. Changes in parameter n and its potential contributors

The n fluctuated noticeably (Fig. 3). Especially in the early 1960s and the late 1980s, the n decreased visibly in many catchments, such as the Tuwei, Dali, Qingjian, Yanhe, Beiluo, Jinghe, Fenhe and Xingshui (Fig. 3).

Records showed that in these two periods, two far-reaching policies were implemented, the "Great Leap Forward" (started in late 1950s) (Song, 2013) and the "Collective Forest Tenure Reform" (in the 1980s)
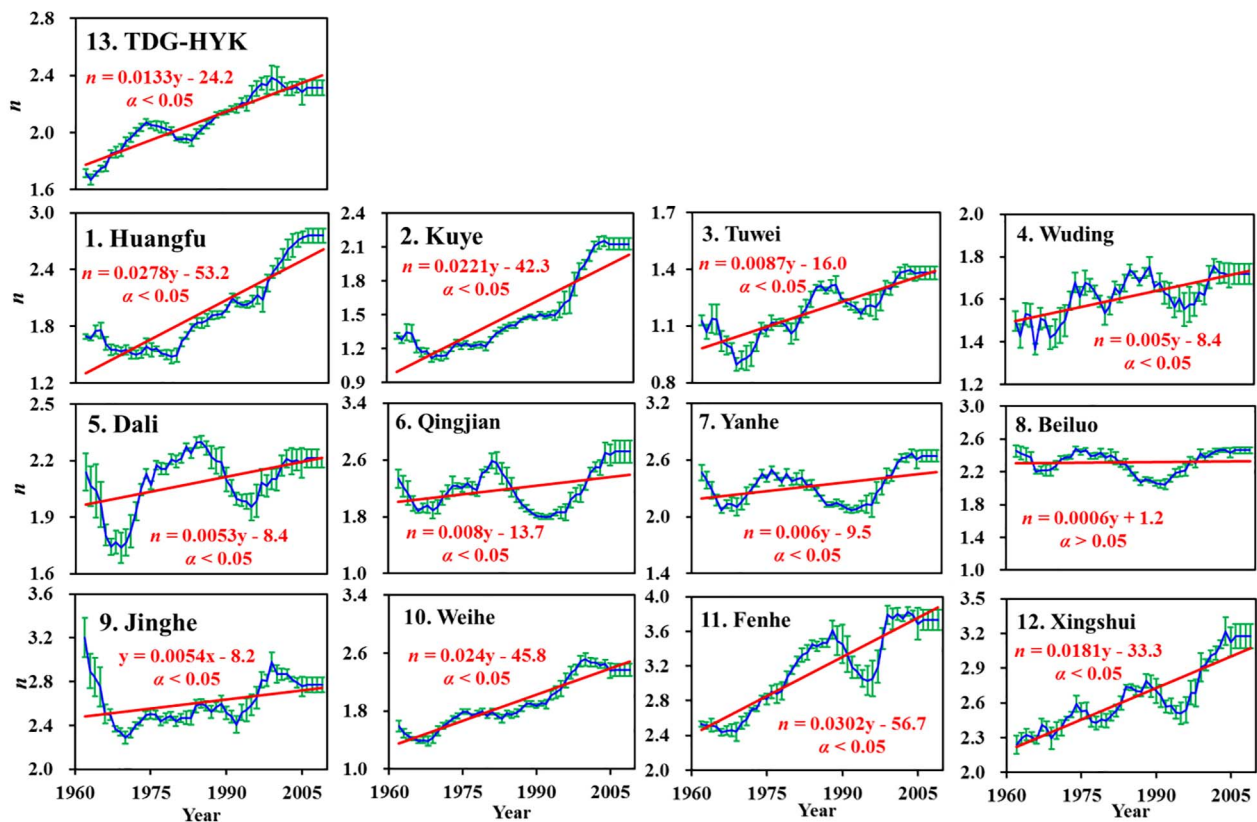
Fig. 3. Time series of dynamic n, the blue line is the mean of the 6 n series (the n_d^5, n_d^6, n_d^7, n_d^8, n_d^9, and n_d^{10}), the green error bars represent the standard deviation of the 6 n series, and the red line is the linear trend. (For interpretation of the references to colour in this figure legend, the reader is referred to the web version of this article.)

(Li, 2011). These two policies had led to large-scale deforestation over China, including the LP (http://www.forestry.gov.cn/Zhuanti/content_lqgg/433963.html) (Sang, 2005). For example in Gansu province, about $1.5 \times 10^4 \, hm^2$ of shelter forest was felled during 1957–1960 ("Great Leap Forward") (http://view.news.qq.com/original/legacyintouch/d602.html). In the Jinghe catchment, where the n dropped sharply before 1970s and increased gradually since then (Fig. 3), the forest coverage on Ziwu mountain (located in the eastern part of Jinghe catchment) decreased by 40.0% during 1950s–1980s (Sang, 2005) and started to increase (exactly the vegetation cover) since the late 1990 s (Xie et al., 2009). Nevertheless, the parameter n exhibited overall significantly increasing trends ($\alpha < 0.05$), especially after the late 1990s, when the "Grain-for-Green" project started (Fig. 3). The mean trend of n in these catchments was $(1.34 \pm 0.99) \times 10^{-2}$ year^{-1}.

Table 2 presents the correlations between the parameter n and land surface properties. Clearly, the n in all the catchments except the Qingjian (No. 6), Beiluo (No. 8) and TDG-HYK (No. 13), were significantly correlated to one or more of the land surface properties. For example, the n in the Huangfu catchment (No. 1) was significantly ($\alpha < 0.05$) correlated to the LIM (0.88), RM (0.84) and LAI (0.99), and the n in the Wuding catchment (No. 4) was significantly ($\alpha < 0.05$) correlated to RM (0.93). Note that in the Qingjian (No. 6), Beiluo (No. 8) and TDG-HYK (No. 13) catchment, there also existed relatively high correlations (> 0.60) though they were not significant (Table 2).

3.2. Temporal patterns of the SWI_c and SWI_{cl}

Noticeable differences existed between SWI_{cl} and SWI_c (Fig. 4). Generally, the SWI_{cl} coincided with the SWI_c in the early years and diverged later, especially after the 1990s (Fig. 4).

Table 2
Correlation coefficients among the parameter n, area of land improvement measures, area of replanted trees and pastures, leaf area index and vegetation coverage in the 13 catchments.

No.	Correlation				No.	Correlation			
	LIM[1]	RM[2]	LAI[3]	VC[4]		LIM	RM	LAI	VC
1	0.88[*,5]	0.84[*]	0.99[*]	0.24	8	0.36	0.38	0.60	0.24
2	0.97[*]	0.99[*]	0.96[*]	−0.05	9	0.99[*]	0.99[*]	0.85[*]	0.93[*]
3	0.94[*]	0.98[*]	0.79	0.32	10	0.98[*]	0.76	0.95[*]	0.88[*]
4	0.75	0.93[*]	−0.26	−0.21	11	0.33	0.97[*]	0.54	0.53
5	0.43	0.40	0.83	0.99[*]	12	0.94[*]	0.94[*]	0.68	0.72
6	0.61	0.54	0.78	−0.26	13	_[5]	–	0.23	0.77
7	0.63	0.56	0.87[*]	0.65					

[6][*] means the correlation is significant at $\alpha = 0.05$.
[1] Land improvement measures including terrace and check dams.
[2] Replanting trees and pastures.
[3] Leaf area index.
[4] Vegetation coverage.
[5] The LIM and RM are not available in TDG-HYK.

The mean absolute differences between SWI_{cl} and SWI_c were 0.21 ± 0.16 and 0.37 ± 0.28, respectively, in the periods of 1961–1990 and 1991–2009. Meanwhile, the trends in SWI_c and SWI_{cl} were negative in all the catchments (Fig. 5). Furthermore, the (negative) trends in SWI_{cl} were visibly larger than those in SWI_c in all the catchments (Fig. 5). The mean trend of SWI_c and SWI_{cl} in the 12 tributaries were $(-1.3 \pm 0.65) \times 10^{-3}$ month^{-1} and $(-2.7 \pm 0.76) \times 10^{-3}$ month^{-1}, respectively. While in the TDG-HYK, which covers the major part of the LP, the trends of SWI_c and SWI_{cl} were -1.6×10^{-3} month^{-1} and $(-3.5 \pm 0.06) \times 10^{-3}$ month^{-1}, respectively.
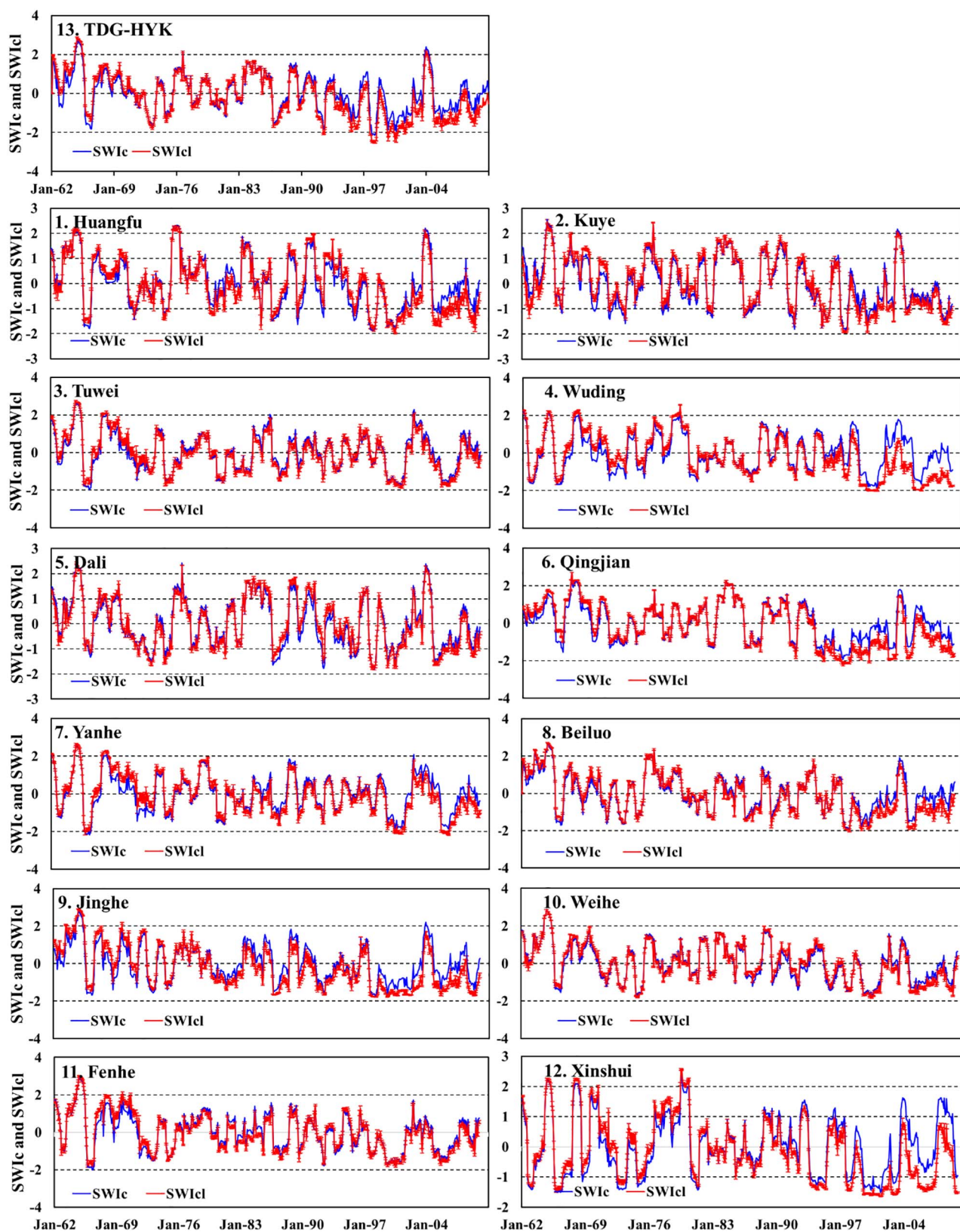
Fig. 4. Time series of *SWI*$_c$ and the *SWI*$_{cl}$ in the 13 catchments; the red error bars are the standard deviation of the 6 *SWI*$_{cl}$ series. (For interpretation of the references to colour in this figure legend, the reader is referred to the web version of this article.)
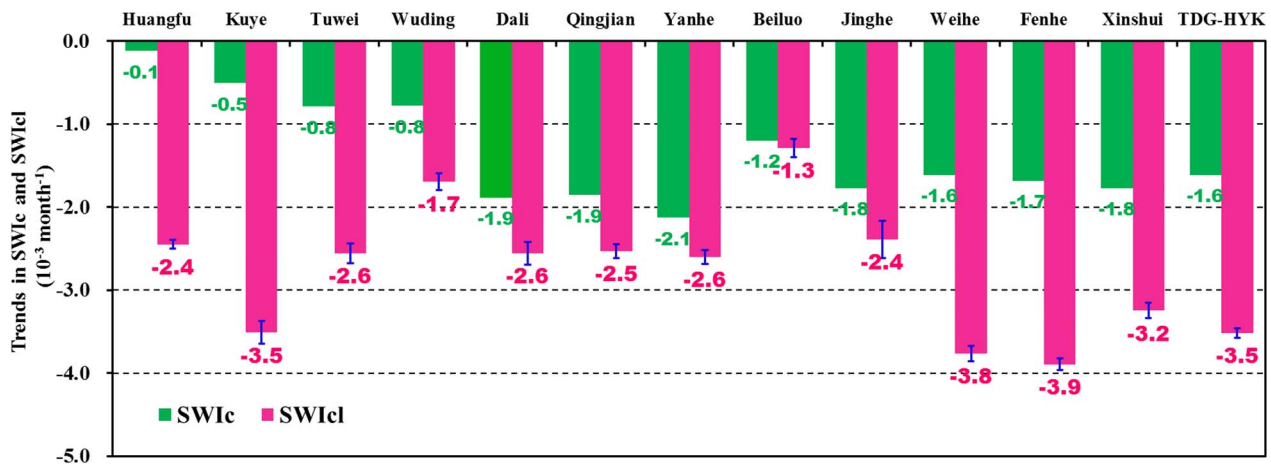
Fig. 5. Trends in *SWI_c* and *SWI_cl*, the blue error bars are the standard deviation of the trends of the 6 *SWI_cl* series. (For interpretation of the references to colour in this figure legend, the reader is referred to the web version of this article.)
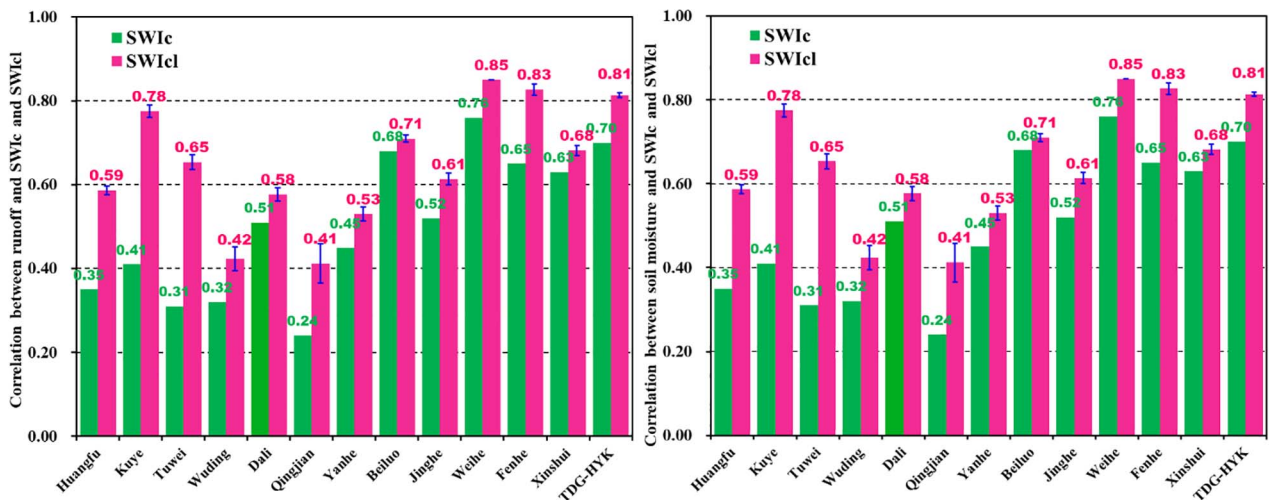

Fig. 6. Correlation among annual mean drought indices, runoff and soil moisture.

3.3. Comparisons of SWI_c and SWI_cl in runoff and soil moisture indication

Fig. 6 shows the correlations among the annual runoff (*Q*), annual mean soil moisture (*SM*), annual mean SWI_c and SWI_{cl} (SWI_{cl5}, SWI_{cl6}, SWI_{cl7}, SWI_{cl8}, SWI_{cl9}, and SWI_{cl10}). Clearly, the correlations for SWI_{cl} vs. *Q* were higher than those for the SWI_c vs. *Q* in all the catchments. The mean correlation for SWI_{cl} vs. *Q* was 0.65 ± 0.14 and that for SWI_c vs. *Q* was 0.50 ± 0.17. Similarly, the correlations for SWI_{cl} vs. *SM* (mean of 0.53 ± 0.10) were obviously higher than those for SWI_c vs. *SM* (mean of 0.43 ± 0.10) (Fig. 6).

4. Discussion

Large scale ecological restoration (ER) activities in the LP have noticeably improved vegetation and reduced soil erosion (Wang et al., 2015b; Zhang et al., 2016a). However, modified land surface (land cover changes) have important roles on water balance (Gao et al., 2014; Liu et al., 2016b; Zhang et al., 2016b). Especially in the water limited regions ($P/ET_0 < 1$) like LP, land cover changes may lead to greater hydrological responses (Zhou et al., 2015). Recently, many studies pointed out that the ER activities contributed to major part of the reduction in runoff (Liang et al., 2015; Zhang et al., 2014, 2008a,b). However, besides runoff, altered water-energy balance can also change the dry and wet conditions, which may be more critical for the local

ecological environment. This study try to evaluate the impacts of land surface changes on the drying tendencies over the LP, by using a newly developed standardized wetness index (*SWI*). The SWI can be used to quantify the hydrological dryness/wetness resulting from climate change (variability) solely (SWI_c), and from the joint effects of climate and land surface changes (variability) (SWI_{cl}) (Liu et al., 2017).

Results showed that in the 13 tributaries in the LP, the parameter *n* in the Choudhury's equation (Choudhury, 1999), generally exhibited significant ($\alpha < 0.05$) increasing trends with noticeable fluctuation in the past decades (mean trend was $(1.34 \pm 0.99) \times 10^{-2}\,\text{year}^{-1}$) (Fig. 3). Increasing *n* indicated that more water would be evaporated from precipitation under a given climate. This is evidenced by the decreasing runoff coefficient over the LP (Liang et al., 2015; Tian et al., 2016; Zhao and Yu, 2013).

Moreover, the parameter *n* is closely related to one or more the land surface properties (*LIM*, *RM*, *VC* and *LAI*), with correlations being mainly higher than 0.8 (Table 2). Meanwhile, the decreases in *n* in many tributaries in the 1950s and 1980s (Fig. 3), within which two national policies that led to large scale deforestation were implemented, also supported the importance of land surface changes in the behaviors of *n*. Exactly, many studies reported close relationships between parameter *n* (or ω in Fu's equation (Fu, 1981)) and catchment properties. For example, Liang et al. (2015) found that the *n* was highly correlated to the total percentage of the affecting area of terraces, trees,

pastures and check-dams in catchments over the LP; Zhang et al. (2016b) established a relationship linking the changes in n and fPAR (fraction of Photosynthetically Active Radiation absorbed by vegetation). In fact, the n in the Choudhury's equation (Choudhury, 1999) is not only affected by the land surface properties, but also affected by climate seasonality (Chen et al., 2013; Donohue et al., 2007, 2010; Hickel and Zhang, 2006). In the same region, Ning et al. (2017) found that the ω (in Fu's equation) was well correlated to the vegetation coverage and climate seasonality; however, the correlation for ω vs. climate seasonality ($R^2 = 0.24$) (Woods, 2003) was obviously lower than that for ω v.s. vegetation coverage ($R^2 = 0.43$). Meanwhile, besides the factors mentioned above, human water consumption would also have a role in affecting the increasing n, because in this paper, the evaporation was estimated by $P-Q$ (Eq. (6)). However, data showed that the human water consumption accounts for a very small part of the precipitation (~1.0%) in this region (Wang et al., 2002). Therefore, it is reasonable to believe that the changes in n were dominated by land surface changes over the LP.

Owing to the climate and land surface change, both the static n based SWI_c and the dynamic n based SWI_{cl} showed decreasing tendencies (Figs. 4 and 5), suggesting that the LP was becoming drier. This is in agreement with the findings based on other drought indices (Zhang et al., 2016a; Zhao and Wu, 2013). Most importantly, the trends in SWI_{cl} (mean of $(-2.7 \pm 0.76) \times 10^{-3}\,\mathrm{month}^{-1}$) were larger than those in SWI_c (mean of $(-1.3 \pm 0.65) \times 10^{-3}\,\mathrm{month}^{-1}$) (Fig. 5). The larger negative trends in SWI_{cl}, together with the fact that land surface changes controlled the changes in n (Table 2), indicated that land surface changes might have enhanced the drying tendencies (hydrological) in this region.

Land surface changes over the LP are mainly due to the implemented large scale ER activities. The ER activities not only improved water conservation (retain more precipitation in the catchment and reduce runoff, through canopy interception, soil water infiltration and groundwater recharge) (Zhang et al., 2014), but also increased ecological water consumption. Under a given climate (precipitation), increasing ecological water consumption would reduce Q, but would not always result in drier environment (e.g. lower soil moisture). For instant, if the increase in infiltration due to ER activities can't compensate the increase in ecological water consumption, then a drier environment would be resulted in. However, if the increase in infiltration can compensate fully the increase in water consumption, then the ER activities may have no (or very slight) effects on drying the local environment. From this perspective, the results above indicated that the ER activities over the LP had increased ecological water consumption (evapotranspiration) more significantly than infiltration. This is indirectly demonstrated by the widely distributed 'little old man trees' (Chen et al., 2015; Liang et al., 2006) and 'dried soil layer' (Wang et al., 2010, 2009). Because that the increased infiltration can't compensate for the increased water consumption, the vegetation, especially the deep rooted plants (such as the poplar tree, which is used as the main species in afforestation over the LP), would extract water from the deep soil layers and bring out dried soil layer (Wang et al., 2010, 2009). In turn, the dried environment limited the vegetation growth, and led to 'little old man trees'. Data showed that during 1979–2014, the annual mean soil moisture (CCI SM) decreased in all the catchments, with the mean trend of $(-3.1 \pm 0.8) \times 10^{-4}\,\mathrm{cm}^3\,\mathrm{cm}^{-3}\,\mathrm{year}^{-1}$.

On the other hand, Q and SM are the consequences of the ecohydrological cycles (water balance), the higher correlation for SWI_{cl} vs. Q (and SM) than those for SWI_c vs. Q (and SM) (Fig. 6), not only indicated that the SWI_{cl} had better effectiveness in indicating hydrological (Q) and agricultural (SM) drought than the SWI_c, but also suggested that the drying tendencies would be more severe than that resulting from meteorological changes solely.

In September 2014, the Chinese government indicated that they planned to expand the "Grain for Green" program (Chen et al., 2015). However, besides the positive effects in reduction of soil erosion and

expansion in vegetation (Wang et al., 2015b), the roles that ER activities play in reduction of runoff and runoff coefficient has been intensively reported (Gao et al., 2015; Liang et al., 2015; Zhang et al., 2014, 2008b; Zhao and Yu, 2013). Reduction in runoff would affect the human society and ecosystems in the lower reaches (Wang et al., 2001). Meanwhile, the results in this study suggested that ER activities (land surface changes) enhanced drying tendencies, indicating that the sustainability of the recovered ecosystem may be not strong under these conditions of climate change and ER strategies. Furthermore, a previous study pointed out that the net primary product over LP has already reached to the limited value, above which the population would suffer water shortages (Feng et al., 2016). Therefore, in future ER designing and management, the policy makers should pay more attention to, and fully assess the eco-hydrological effects of the ER activities.

5. Conclusion

This study evaluated the effects of land surface changes on hydrological dryness in 13 main catchments over China's Loess Plateau (LP) during 1961–2009, by using the standardized wetness index (SWI). The n (a parameter of the Budyko-type formulae) generally increased (overall by $(1.34 \pm 0.99) \times 10^{-2}\,\mathrm{year}^{-1}$) and was significantly ($\alpha < 0.05$) correlated to the land surface properties (one or more, correlations were generally higher than 0.8), including the land improvement measures (LIM, total affecting area of terrace and check dams), replanting measures (RM, total affecting area of replanted trees and pastures), LAI (leaf area index), and VC (vegetation coverage). These indicated that the land surface changes dominated the behaviors of n over the LP. Moreover, both the SWI_c and SWI_{cl} exhibited downward trends, while the (negative) trends in SWI_{cl} (mean of $(-2.7 \pm 0.76) \times 10^{-3}\,\mathrm{month}^{-1}$) were noticeably larger than those in SWI_c (mean of $(-1.3 \pm 0.65) \times 10^{-3}\,\mathrm{month}^{-1}$) in all the catchments. These findings suggested that the LP was drying (decreasing SWI_c), however, the land surface changes, which are mainly related to ecological restoration measures, enhanced the drying tendencies. Therefore, the Chinese government needs to fully consider the eco-hydrological effects of the ER activities in future water resources management and ecological reconstruction related policy making.

References

Allen, R.G., Pereira, L.S., Raes, D., Smith, M., 1998. Crop Evapotranspiration: Guidelines for Computing Crop Water Requirements. Food and Agriculture Organization of the United Nations, Rome.

Anyamba, A., Small, J.L., Tucker, C.J., Pak, E.W., 2014. Thirty-two years of sahelian zone growing season non-stationary NDVI3g patterns and trends. Remote Sens. Basel 6, 3101–3122.

Budyko, M.I., 1974. Climate and Life, english ed. Academic, San Diego, Calif.

Burn, D.H., Elnur, M.A.H., 2002. Detection of hydrologic trends and variability. J. Hydrol. 255, 107–122.

Chen, X., Alimohammadi, N., Wang, D.B., 2013. Modeling interannual variability of seasonal evaporation and storage change based on the extended Budyko framework. Water Resour. Res. 49, 6067–6078 6010.1002/Wrcr.20493.

Chen, Y.P., Wang, K.B., Lin, Y.S., Shi, W.Y., Song, Y., He, X.H., 2015. Balancing green and grain trade. Nat. Geosci. 8, 739–741.

Choudhury, B.J., 1999. Evaluation of an empirical equation for annual evaporation using

field observations and results from a biophysical model. J. Hydrol. 216, 99–110.

Dai, A.G., 2011. Drought under global warming: a review. Wires Clim. Change 2, 45–65.

Donohue, R.J., Roderick, M.L., McVicar, T.R., 2007. On the importance of including vegetation dynamics in Budyko's hydrological model. Hydrol. Earth Syst. Sci. 11, 983–995.

Donohue, R.J., Roderick, M.L., McVicar, T.R., 2010. Can dynamic vegetation information improve the accuracy of Budyko's hydrological model? J. Hydrol. 390, 23–34.

Donohue, R.J., Roderick, M.L., McVicar, T.R., Farquhar, G.D., 2013. Impact of CO_2 fertilization on maximum foliage cover across the globe's warm, arid environments. Geophys. Res. Lett. 40, 3031–3035.

Feng, X.M., Sun, G., Fu, B.J., Su, C.H., Liu, Y., Lamparski, H., 2012. Regional effects of vegetation restoration on water yield across the Loess Plateau, China. Hydrol. Earth Syst. Sci. 16, 2617–2628.

Feng, X.M., Fu, B.J., Piao, S.L., Wang, S., Ciais, P., Zeng, Z.Z., Lü, Y.H., Zeng, Y., Li, Y., Jiang, X.H., Wu, B.F., 2016. Revegetation in China's Loess Plateau is approaching sustainable water resource limits. Nat. Clim. Change. http://dx.doi.org/10.1038/NCLIMATE3092.

Fu, B.P., 1981. On the calculation of the evaporation from land surface (in Chinese). Sci. Atmos. Sin. 5, 23–31.

Gao, H., Hrachowitz, M., Schymanski, S.J., Fenicia, F., Sriwongsitanon, N., Savenije, H.H.G., 2014. Climate controls how ecosystems size the root zone storage capacity at catchment scale. Geophys. Res. Lett. 41, 7916–7923.

Gao, P., Jiang, G.T., Wei, Y.P., Mu, X.M., Wang, F., Zhao, G.J., Sun, W.Y., 2015. Streamflow regimes of the Yanhe River under climate and land use change, Loess Plateau, China. Hydrol. Process. 29, 2402–2413.

Hickel, K., Zhang, L., 2006. Estimating the impact of rainfall seasonality on mean annual water balance using a top-down approach. J. Hydrol. 331, 409–424 410.1016/j.jhydrol.2006.1005.1028.

Kendall, M.G., 1975. Rank Correlation Methods. Charles Griffin, London.

Li, Z., 2011. Evaluation and thought on the collective forest tenure reform. For. Econ. Rev. 1, 33–41.

Li, D., Pan, M., Cong, Z.T., Zhang, L., Wood, E., 2013. Vegetation control on water and energy balance within the Budyko framework. Water Resour. Res. 49, 969–976.

Liang, W., Bai, D., Wang, F.Y., Fu, B.J., Yan, J.P., Wang, S., Yang, Y.T., Long, D., Feng, M.Q., 2015. Quantifying the impacts of climate change and ecological restoration on streamflow changes based on a Budyko hydrological model in China's Loess Plateau. Water Resour. Res. 51, 6500–6519.

Liang, Z.S., Yang, H.W., Shao, H.B., Han, R.L., 2006. Investigation on water consumption characteristics and water use efficiency of poplar under soil water deficits on the Loess Plateau. Colloid Surf. B 53, 23–28.

Liu, Q., McVicar, T.R., Yang, Z.F., Donohue, R.J., Liang, L.Q., Yang, Y.T., 2016b. The hydrological effects of varying vegetation characteristics in a temperate water-limited basin: development of the dynamic Budyko-Choudhury-Porporato (dBCP) model. J. Hydrol. 543, 595–611.

Liu, M.X., Xu, X.L., Wang, D.B., Sun, A.Y., Wang, K.L., 2016a. Karst catchments exhibited higher degradation stress from climate than the non-karst catchments in southwest China: an ecohydrological perspective. J. Hydrol. 535, 173–180.

Liu, M.X., Xu, X.L., Xu, C.H., Sun, A.Y., Wang, K.L., Scanlon, B.R., Zhang, L., 2017. A new drought index that considers the joint effects of climate and land surface change. Water Resour. Res. http://dx.doi.org/10.1002/2016WR020178.

Mann, H.B., 1945. Nonparametric tests against trend. Econometrica 13, 245–259.

McKee, T.B., Doesken, N.J., Kleist, J., 1993. The relationship of drought frequency and duration to time scales. In: Eighth Conf. on Applied Climatology. Amer. Meteor. Soc., Anaheim, CA, pp. 179–184.

McVicar, T.R., Li, L., Van Niel, T.G., Zhang, L., Li, R., Yang, Q., Zhang, X., Mu, X., Wen, Z., Liu, W., Zhao, Y., Liu, Z., Gao, P., 2007a. Developing a decision support tool for China's re-vegetation program: simulating regional impacts of afforestation on average annual streamflow in the Loess Plateau. For. Ecol. Manage. 251, 65–81.

McVicar, T.R., Van Niel, T.G., Li, L.T., Hutchinson, M.F., Mu, X.M., Liu, Z.H., 2007b. Spatially distributing monthly reference evapotranspiration and pan evaporation considering topographic influences. J. Hydrol. 338, 196–220.

Ning, T.T., Li, Z., Liu, W.Z., 2017. Vegetation dynamics and climate seasonality jointly control the interannual catchment water balance in the Loess Plateau under the Budyko framework. Hydrol. Earth Syst. Sci. 21, 1515–1526.

Palmer, W.C., 1965. Meteorological Drought. Research Paper, 45. U.S. Weather Bureau, Washington, D.C., pp. 58.

Penman, H.L., 1948. Natural evaporation from open water, bare soil and grass. Proc. R. Soc. Lond. A 193, 120–145.

Sang, G.S., 2005. Vegetation variation of loess plateau during human history. J. Arid Land Resour. Environ. 19, 54–58.

Song, S.G., 2013. Identifying the intergenerational effects of the 1959–1961 Chinese Great Leap Forward Famine on infant mortality. Econ. Hum. Biol. 11, 474–487.

Tian, P., Zhai, J.Q., Zhao, G.J., Mu, X.M., 2016. Dynamics of runoff and suspended sediment transport in a highly erodible catchment on the Chinese Loess Plateau. Land Degrad. Dev. 27, 839–850.

Vicente-Serrano, S.M., Begueria, S., Lopez-Moreno, J.I., 2010. A multiscalar drought index sensitive to global warming: the standardized precipitation evapotranspiration

index. J. Clim. 23, 1696–1718.

Vicente-Serrano, S.M., Lopez-Moreno, J.I., 2005. Hydrological response to different time scales of climatological drought: an evaluation of the standardized precipitation index in a mountainous Mediterranean basin. Hydrol. Earth Syst. Sci. 9, 523–533.

Wang, Y., Arrhenius, G., Zhang, Y.Z., 2001. Drought in the Yellow River – an environmental threat to the coastal zone. In: Journal of Coastal Research Special Issue 34, International Coastal Symposium (ICS 2000): Challenges for the 2021st Century in Coastal Sciences, Engineering and Environment (August 2001), pp. 2503–2515.

Wang, G., Fan, Z., 2002. In: Variation of Streamflow and Sediment Flux in the Yellow River (in Chinese). Yellow River Conserv. Press, Zhengzhou, China, pp. 351–531.

Wang, S., Fu, B.J., Piao, S.L., Lü, Y.H., Ciais, P., Feng, X.M., Wang, Y.F., 2015b. Reduced sediment transport in the Yellow River due to anthropogenic changes. Nat. Geosci. http://dx.doi.org/10.1038/NGEO2602.

Wang, Z.Q., Liu, B.Y., Liu, G., Zhang, Y.X., 2009. Soil water depletion depth by planted vegetation on the Loess Plateau. Sci. China. Ser. D 52, 835–842.

Wang, Y.Q., Shao, M.A., Shao, H.B., 2010. A preliminary investigation of the dynamic characteristics of dried soil layers on the Loess Plateau of China. J. Hydrol. 381, 9–17.

Wang, Y.M., Zhang, X.C., Wang, L., Zhou, J.B., 2002. Analysis of changes in natural runoff in the Yellow River Basin in 1990s. Yellow River 24, 9–12.

Wang, L.N., Zhu, Q.K., Zhao, W.J., Zhao, X.K., 2015a. The drought trend and its relationship with rainfall intensity in the Loess Plateau of China. Nat. Hazards 77, 479–495.

Woods, R., 2003. The relative roles of climate, soil, vegetation and topography in determining seasonal and long-term catchment dynamics. Adv. Water Resour. 26, 295–309.

Xie, F., Qiu, G.Y., Yin, J., Xiong, Y.J., Wang, P., 2009. Comparison of land use/land cover change in three sections of the Jinghe river basin between the 1970s and 2006. J. Nat. Resour. 24, 1354–1365.

Yang, Y.T., Donohue, R.J., McVicar, T.R., Roderick, M.L., Beck, H.E., 2016. Long-term CO_2 fertilization increases vegetation productivity and has little effect on hydrological partitioning in tropical rainforests. J. Geophys. Res. Biogeosci. 121, 2125–2140.

Yang, H.B., Qi, J., Xu, X.Y., Yang, D.W., Lv, H.F., 2014. The regional variation in climate elasticity and climate contribution to runoff across China. J. Hydrol. 517, 607–616 610.1016/j.jhydrol.2014.1005.1062.

Yao, W.Y., Xu, J.H., Ran, D.C., 2011. In: Assessment of Changing Trends in Streamflow and Sediment Fluxes in the Yellow River Basin (in Chinese). Yellow River Conserv. Press, Zhengzhou, China, pp. 25–36.

Yue, S., Wang, C.Y., 2002. Applicability of prewhitening to eliminate the influence of serial correlation on the Mann-Kendall test. Water Resour. Res. 38. http://dx.doi.org/10.1029/2001WR000861.

Zeng, C., Shao, M.A., Wang, Q.J., Zhang, J., 2011. Effects of land use on temporal-spatial variability of soil water and soil-water conservation. Acta Agric. Scand. B 61, 1–13.

Zhang, B.Q., Wu, P.T., Zhao, X.N., Wang, Y.B., Wang, J.W., Shi, Y.G., 2012. Drought variation trends in different subregions of the Chinese Loess Plateau over the past four decades. Agric. Water Manage. 115, 167–177.

Zhang, B.Q., Wu, P.T., Zhao, X.N., Wang, Y.B., Gao, X.D., Cao, X.C., 2013. A drought hazard assessment index based on the VIC-PDSI model and its application on the Loess Plateau, China. Theor. Appl. Climatol. 114, 125–138.

Zhang, B.Q., He, C.S., Burnham, M., Zhang, L.H., 2016a. Evaluating the coupling effects of climate aridity and vegetation restoration on soil erosion over the Loess Plateau in China. Sci. Total Environ. 539, 436–449.

Zhang, L.L., Podlasly, C., Ren, Y., Feger, K.H., Wang, Y.H., Schwarzel, K., 2014. Separating the effects of changes in land management and climatic conditions on long-term streamflow trends analyzed for a small catchment in the Loess Plateau region, NW China. Hydrol. Process. 28, 1284–1293.

Zhang, S.L., Yang, H.B., Yang, D.W., Jayawardena, A.W., 2016b. Quantifying the effect of vegetation change on the regional water balance within the Budyko framework. Geophys. Res. Lett. 43, 1140–1148.

Zhang, X.P., Zhang, L., McVicar, T.R., Van Niel, T.G., Li, L.T., Li, R., Yang, Q.K., Wei, L., 2008a. Modelling the impact of afforestation on average annual streamflow in the Loess Plateau, China. Hydrol. Process. 22, 1996–2004.

Zhang, X.P., Zhang, L., Zhao, J., Rustomji, P., Hairsine, P., 2008b. Responses of streamflow to changes in climate and land use/cover in the Loess Plateau, China. Water Resour. Res. 44.

Zhao, M.S., Running, S.W., 2010. Drought-induced reduction in global terrestrial net primary production from 2000 through 2009. Science 329, 940–943.

Zhao, G.J., Tian, P., Mu, X.M., Jiao, J.Y., Wang, F., Gao, P., 2014. Quantifying the impact of climate variability and human activities on streamflow in the middle reaches of the Yellow River basin, China. J. Hydrol. 519, 387–398.

Zhao, X.N., Wu, P., 2013. Meteorological drought over the Chinese Loess Plateau: 1971–2010. Nat. Hazards 67, 951–961.

Zhao, Y., Yu, X.X., 2013. Effects of climatic variability and human activity on runoff in the Loess Plateau of China. For. Chron 89, 153–161.

Zhou, G.Y., Wei, X.H., Chen, X.Z., Zhou, P., Liu, X.D., Xiao, Y., Sun, G., Scott, D.F., Zhou, S.Y.D., Han, L.S., Su, Y.X., 2015. Global pattern for the effect of climate and land cover on water yield. Nat. Commun. 6.